Guiding magnetic liquid metal for flexible circuit

OPEN ACCESS
IOP Publishing | IMMT
International Journal of Extreme Manufacturing
Int. J. Extrem. Manuf. **3** (2021) 025102 (10pp)
https://doi.org/10.1088/2631-7990/abeda3

Guiding magnetic liquid metal for flexible circuit

Chengjun Zhang[1,3], Qing Yang[1,3,*], Jiale Yong[2,3], Chao Shan[2,3], Jingzhou Zhang[2,3], Xun Hou[2,3] and Feng Chen[2,3,*]

[1] School of Mechanical Engineering, Xi'an Jiaotong University, Xi'an 710049, People's Republic of China
[2] State Key Laboratory for Manufacturing System Engineering and Shaanxi Key Laboratory of Photonics Technology for Information, School of Electronics and Information Engineering, Xi'an Jiaotong University, Xi'an 710049, People's Republic of China
[3] The International Joint Research Laboratory for Micro/Nano Manufacturing and Measurement Technologies, Xi'an Jiaotong University, Xi'an 710049, People's Republic of China

E-mail: chenfeng@mail.xjtu.edu.cn and yangqing@mail.xjtu.edu.cn

Received 20 January 2021, revised 15 February 2021
Accepted for publication 10 March 2021
Published 6 April 2021

Abstract

Liquid metal (LM) has potential applications in flexible electronics due to its high electrical conductivity and high flexibility. However, common methods of printing LM circuits on soft substrates lack controllability, precision, and the ability to repair a damaged circuit. In this paper, we propose a method that uses a magnetic field to guide a magnetic LM (MLM) droplet to print and repair a flexible LM circuit on a femtosecond (fs) laser-patterned silicone surface. After mixing magnetic iron (Fe) particles into LM, the movement of the resultant MLM droplet could be controlled by a magnetic field. A patterned structure composed of the untreated flat domain and the LM-repellent rough microstructure produced by fs laser ablation was prepared on the silicone substrate. As an MLM droplet was guided onto the designed pattern, a soft LM circuit with smooth, uniform, and high-precision LM lines was obtained. Interestingly, the MLM droplet could also be guided to repair the circuit broken LM lines, and the repaired circuit maintained its original electrical properties. A flexible tensile sensor was prepared based on the printed LM circuit, which detected the bending degree of a finger.

Supplementary material for this article is available online

Keywords: liquid metal, flexible circuit, femtosecond laser, magnetic control, supermetalphobic microstructure

1. Introduction

Flexible electronic devices with integrated electronic components on flexible materials attract increasing interest because of their wide applications in health monitoring, medical treatment, biological studies, and so on [1–7]. Flexible conductors were previously prepared by combining conductive fillers and stretchable elastomers. For example, metal nanoparticles, metal nanowires, and ionic gel were embedded into an elastomer to form a conductive elastomer with good conductivity under strain [8–12]. Recently, liquid metal (LM) has been used as an intrinsically flexible electrode material in the preparation of flexible electronic devices [13–26]. LM, such as eutectic gallium indium (EGaIn), which is liquid at room temperature. Such an LM has desirable characteristics, such

* Authors to whom any correspondence should be addressed.

as good electrical and thermal conductivity, low melting point (<30 °C), non-toxicity, high flexibility, low vapor pressure, and unique surface chemistry [27–36]. As an emerging soft conductive material, LM has great potential in medical treatment [37], flexible wearable equipment [20, 21, 26, 38], health monitoring [39, 40], soft robotics [41], etc. To prepare an LM-based flexible electronic device, the key is integrating the LM on a flexible substrate. Because of the liquid state, the process of printing LM is very different from the conventional rigid metal integrating technology. Some methods have been proposed to print LM on a flexible substrate [42–47]. For example, Liu *et al* directly printed LM ink on the surfaces of various flexible substrates by a two-dimensional printer [42, 43]. Cheng *et al* simply patterned LM and obtained an LM circuit by laser scanning the LM particles [44]. Wang *et al* used the stencil printing method to integrate LM on a flexible substrate [45]. Javey *et al* injected the LM into a designed microchannel in the polydimethylsiloxane (PDMS) and prepared a diaphragm pressure sensor for health and tactile touch monitoring [21]. However, the previously reported methods of printing LM circuits on soft substrates are still restricted by many limitations, such as low controllability, low printing precision, and the inability to repair LM patterns. Some methods were proposed to improve the response of LM to external stimulation to achieve functional control. For example, magnetic components were previously added to the LM to realize LM pattern printing and repair [40, 48], but a size controllable, high-precision, and uniform LM pattern was not be obtained.

Our proposed method uses a magnetic field to guide a magnetic LM (MLM) droplet to print and repair a flexible LM circuit on a femtosecond (fs) laser-patterned silicone surface. During this printing process, a high-precision and uniform LM pattern with different sizes and different line widths can be easily printed according to the design patterns. By tuning the wettability of the LM with an fs laser, the manipulation of the LM will not be hindered by the existence of an oxide layer. An MLM was prepared by mixing iron (Fe) particles into LM. A magnetic field controlled the movement of the resulting MLM. The MLM tightly adhered to the smooth silicone surface. After laser ablation, rough microstructures developed on the silicone substrate, allowing the silicone surface to repel the LM. Like a magnetic-controlled robot, sliding the MLM droplet on the designed pattern easily printed smooth, uniform, and high-precision soft LM circuits on the laser-induced patterns. Interestingly, the magnetic field-controlled MLM droplet was used to repair a broken circuit without affecting the circuit's original electrical properties. The LM circuit was recycled to avoid wasting electronic components and materials (e.g. rigid components, LM, and the silicone substrate). The microstructures on the recycled silicone substrate still maintained acceptable supermetalphobicity, so there was no need to ablate a new circuit pattern. As an example application, a flexible tensile sensor was prepared based on the printed LM circuit to detect the bending degree of a human finger.

2. Experimental section

2.1. Preparation of the MLM composite

The LM used in our experiment was EGaIn (WOCHANG METAL Co., Ltd), which has a melting point of 12 °C. Fe is a typical magnetic material and does not react with LM at room temperature [49]. To endow LM with magnetic properties (responding to the magnetic field), we mixed the LM with some Fe particles. As shown in figure 1(a), a small amount of Fe particles (with a diameter of ∼5 μm) was added to the LM. Then, the mixture was stirred until the Fe particles dispersed uniformly. This process was carried out in an air environment without any chemical treatments.

2.2. Femtosecond laser patterning

As an extreme manufacturing method, fs lasers can achieve high precision and micro/nano scale fabrication [50, 51]. Fs laser ablation has been used to fabricate microstructures on the surface of materials [52, 53]. As shown in figure S1 (supporting information (available online at stacks.iop.org/IJEM/3/025102/mmedia), the silicone sample (MAIJIALONG Co., Ltd) was fixed on a program-controlled moveable stage. An fs laser beam (with a pulse duration of 50 fs, central wavelength of 800 nm, and repetition frequency of 1 kHz) from a Ti:sapphire laser system (Coherent, Libra-usp 1K-he200) was vertically focused onto the surface of the silicone sheet by a plano-convex lens (focal length of 200 mm) in air. A typical line-by-line laser scanning manner was adopted. The laser power, scanning speed, and space/interval of the scanning lines were held constant at 300 mW, 5 mm s^{-1}, and 50 μm, respectively. Only the area surrounding the pattern domain was ablated by laser and thus coated with rough microstructures.

2.3. Printing LM circuit

A magnetic field can control the movement of the MLM because of the presence of magnetic Fe particles in the MLM composite. Figure 2(c) shows the process of guiding an MLM droplet to print LM circuits on the laser-patterned surface. When a magnet-guided MLM droplet moved along the direction of the circuit pattern, a thin layer of LM trace was left on the pattern domain because of the high LM adhesion of the smooth surface and the excellent supermetalphobicity of the laser-structured area. As a result, an LM circuit, which was the same as the designed pattern, formed on the soft silicone surface. Finally, the redundant MLM was removed by a magnet.

2.4. Recycling LM circuit

The LM circuit was soaked in an ethanol solution and cleaned by an ultrasonic cleaner (SHEN CHAO JIE Co., Ltd) at a frequency of 120 KHz for 30 min. The microstructure

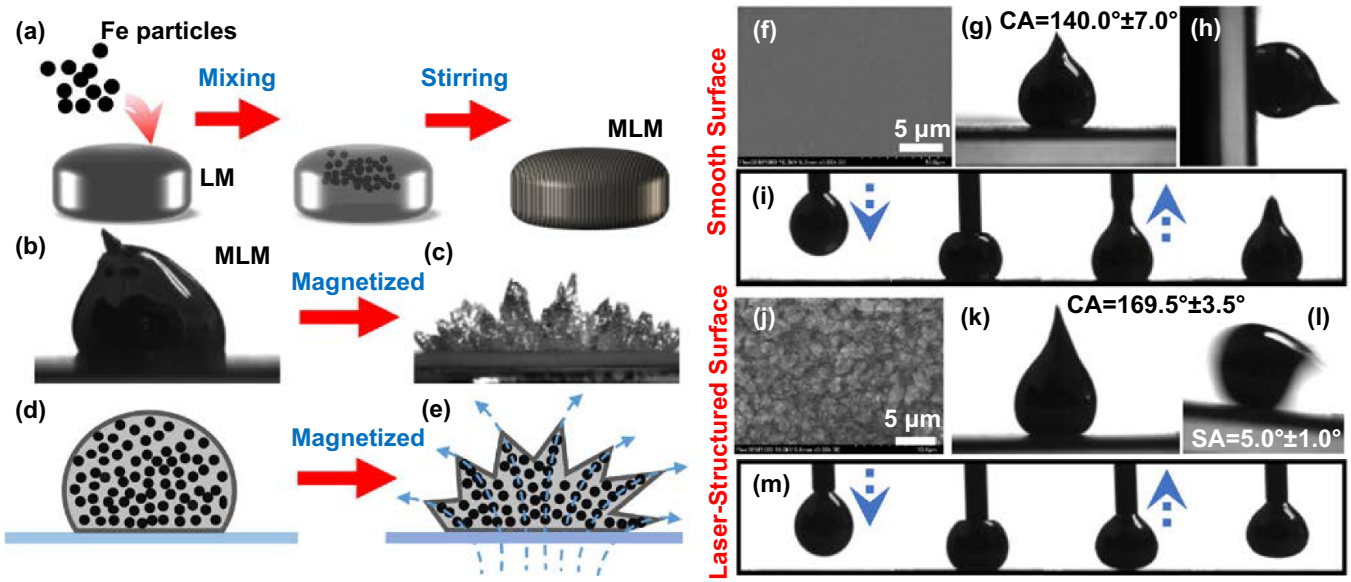

Figure 1. Preparation of an MLM composite and wettability of an MLM droplet on a silicone surface. (a) Process of preparing an MLM. (b) Image of a drop of the as-prepared MLM. (c) Image of the MLM drop under a magnetic field. (d) Model of an MLM droplet. (e) Model of an MLM droplet under a magnetic field. The MLM droplet placed on a silicone surface. (f) SEM image of the untreated smooth silicone surface. (g) An MLM droplet on the smooth silicone surface. (h) An MLM droplet pining on the vertical smooth silicone surface. (i) Process of moving an MLM droplet to touch and then leave the smooth silicone surface. (j) SEM image of the silicone surface after fs laser ablation. (k) An MLM droplet on the laser-structured silicone surface. (l) An MLM droplet rolling on the laser-structured silicone surface tilled at ∼5°. (m) Process of moving an MLM droplet to touch and then leave the laser-structured silicone surface.

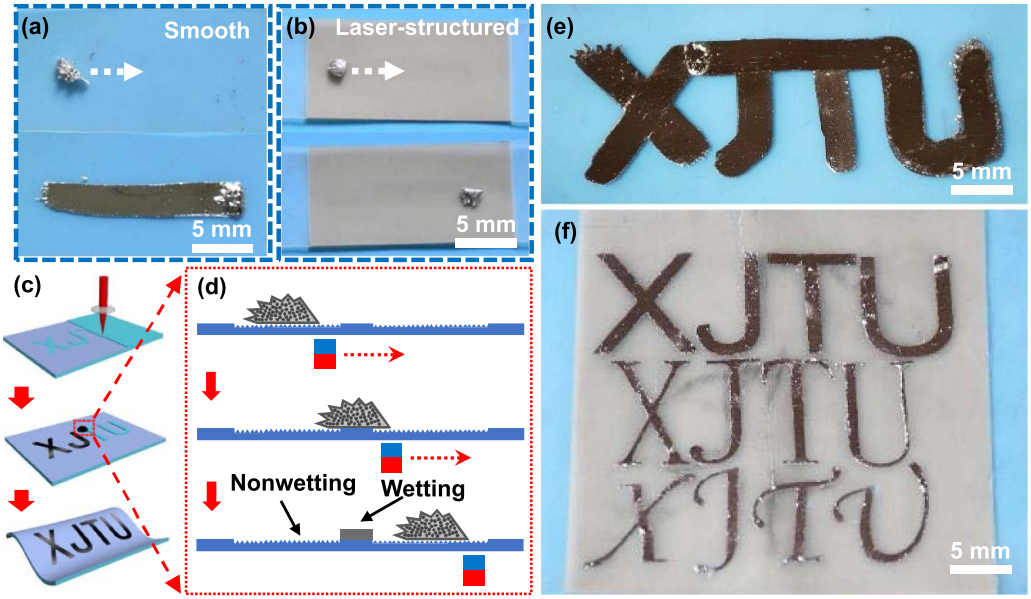

Figure 2. Printing MLM on the laser-patterned surface. (a), (b) Guiding an MLM droplet to move (from left to right) on (a) the smooth silicone surface and (b) the laser-structured silicone surface. (c) Schematic of the process of printing LM on the laser-patterned surface. (d) Mechanism of printing MLM on the smooth domain surrounded by laser-induced microstructures. (e), (f) LM 'XJTU' patterns printed on (e) the smooth surface and (f) the laser-patterned surface.

maintained excellent supermetalphobicity after ultrasonic cleaning, so the laser-pattern could be reused for LM printing.

2.5. Characterization

The surface microstructure of the samples was observed by a Flex 1000 scanning electron microscope (SEM; Hitachi, Japan). The wettability of a liquid EGaIn droplet on the sample surface was investigated by a JC2000D contact angle (CA) system (Powereach, China). The three-dimensional (3D) morphology of the surface of the LM wire was characterized through a LEXT-OLS4000 laser confocal microscope (Olympus, Japan). The resistance of the as-prepared circuit was measured by a multimeter.

3. Results and discussion

An MLM composite was simply prepared by mixing Fe particles into LM (EGaIn), as shown in figure 1(a). First, a small amount of Fe particles (with a diameter of $\sim$5 μm) was added to the LM. Then, the mixture was stirred until the Fe particles dispersed uniformly. The preparation was carried out in an air environment without any chemical treatments. Figure 1(b) shows a drop of the as-prepared MLM on an untreated silicone surface. The MLM droplet has a smooth surface that reflects light. All of the Fe particles are encapsulated within the outer oxide layer of the LM droplet (figure 1(d)). Once a magnetic field was applied to the bottom of the MLM, the MLM droplet formed a mountain-like shape (figure 1(c)) as the internal Fe particles dispersed along the magnetic induction line (figure 1(e)). This result indicates that the MLM responded to the magnetic field, and that its mobility can be flexibly guided by the magnetic field.

The wettability and adhesion of an MLM droplet on a solid substrate is significantly influenced by the surface microstructure of the substrate [54, 55]. Figure 1(f) shows the SEM image of an original untreated silicone surface. The surface is very smooth. When an MLM droplet is dripped onto this surface, the CA of the MLM droplet is measured to be 140.0° $\pm$ 7.0° (figure 1(g)). The MLM droplet firmly adheres to the smooth surface without rolling away even when placed on a vertical surface (figure 1(h)). Figure 1(i) shows the process of moving an MLM droplet to touch and then leave the smooth silicone surface. With lifting the needle, the droplet departs from the needle tube and sticks to the bottom of the silicone substrate. Therefore, the untreated silicone surface shows a high adhesion to the MLM droplet, which results from a large contact area between the MLM and the silicone surface.

Fs laser is a universal method in advanced nano/microfabrication due to its ultra-short pulse width and extremely high peak intensity. These features give the fs laser numerous advantages while ablating a solid substrate, including a small heat-affected zone around the ablation spot, high spatial resolution, extensive material processing, non-contact manufacturing, etc. In our experiment, fs laser processing was utilized to generate microstructures on the surface of a silicone substrate. The fs laser was focused onto the sample surface and then ablated the substrate (figure S1, supporting infroamtion). The fs laser treatment created many particles with sizes ranging from a few hundred nanometers to micrometers on the silicone surface (figure 1(j)). The laser-induced microstructures endowed the silicone surface with supermetalphobicity. The CA of the MLM droplet on the structured surface reached 169.5° $\pm$ 3.5° (figure 1(k)). As long as the sample surface was slightly tilted at 5.0° $\pm$ 1.0°, the MLM droplet quickly rolled away (sliding angle (SA) = 5.0° $\pm$ 1.0°), as shown in figure 1(l). When the MLM droplet was moved to touch and then leave the laser-structured surface, there was no residual on the sample surface, and the MLM droplet was finally taken away by a tube (figure 1(m)). These results reveal that the laser-induced microstructures greatly reduce the adhesion between the MLM and the silicone surface. Such ultralow adhesion resulted from the reduced contact area between the MLM and the structured silicone surface caused by the laser-induced surface microstructures. The MLM only touched the peaks of the microstructures. The limited contact area endowed the laser-treated silicone surface with supermetalphobicity and ultralow adhesion to MLM.

The movement of the MLM can be controlled by a magnetic field because of the presence of magnetic Fe particles in the MLM composite. Figures 2(a) and (b) show the results of an MLM droplet (Fe particles: 15 wt%) being guided forward by a magnet on the untreated silicone surface and laser-structured silicone surface, respectively. A long LM trace was left on the smooth silicone surface behind the MLM droplet due to the high adhesion between the MLM and the silicone substrate (figure 2(a)). The MLM droplet was also controlled to move along a designed path to write LM letters 'XJTU' on the silicon surface, as shown in figure 2(e). However, the printed patterns were disordered and irregular, and the line width, depending on the size of the MLM droplet, was very large. By contrast, the MLM droplet easily rolled onto the laser-structured silicone surface when guided by a magnetic field. There was no LM residue on the path of the MLM droplet (figure 2(b)), which agrees with the supermetalphobicity of the laser-induced structure. Therefore, it was difficult to print the LM on the structured silicone surface, while the LM easily adhered to the untreated silicone surface.

A strategy for printing fine and complicated LM pattern is proposed based on the distinguishing wetting behaviors of the MLM on the smooth surface and the laser-structured surface. As an example, figure 2(c) shows the process of guiding an MLM droplet to print LM 'XJTU' letters on the laser-patterned surface. First, a 'XJTU' pattern was prepared on the surface of the silicone substrate by fs laser selective ablation. The pattern domain was not ablated by laser and stayed smooth. By contrast, the rest of the domain was treated by laser and thus was coated with LM-repellent micro/nanostructures. Then, an MLM droplet was guided by a magnet to print the designed pattern. Because of the high LM adhesion of the smooth domain and the excellent supermetalphobicity of the laser-structured area, only a thin layer of LM trace was left on the pattern domain (figures 2(d) and S2 in the supporting information). As a result, the 'XJTU' pattern coated with LM formed on the soft silicone surface (figure 2(f)). The printed LM patterns were very smooth and uniform (figure S3, supporting information). In the printing process, some gray LM oxide residues may be left on the laser-ablated domain, but these residues do not affect the conductivity of the LM pattern. If the LM is an 'ink', the MLM acts like a writing brush whose movement can be controlled by a magnetic field. Just like writing calligraphy on paper, the LM pattern can be flexibly printed on a soft laser-patterned substrate.

A soft circuit was prepared by printing the MLM on the laser-patterned silicone surface. Figure 3(a) shows the process of preparing an LM conductive line, which is the base in a circuit. The initial circuit pattern was formed by selective fs laser ablation. Then, the LM circuit was obtained by moving the MLM droplet on the laser-patterned surface. The content of Fe particle in the MLM has a significant influence

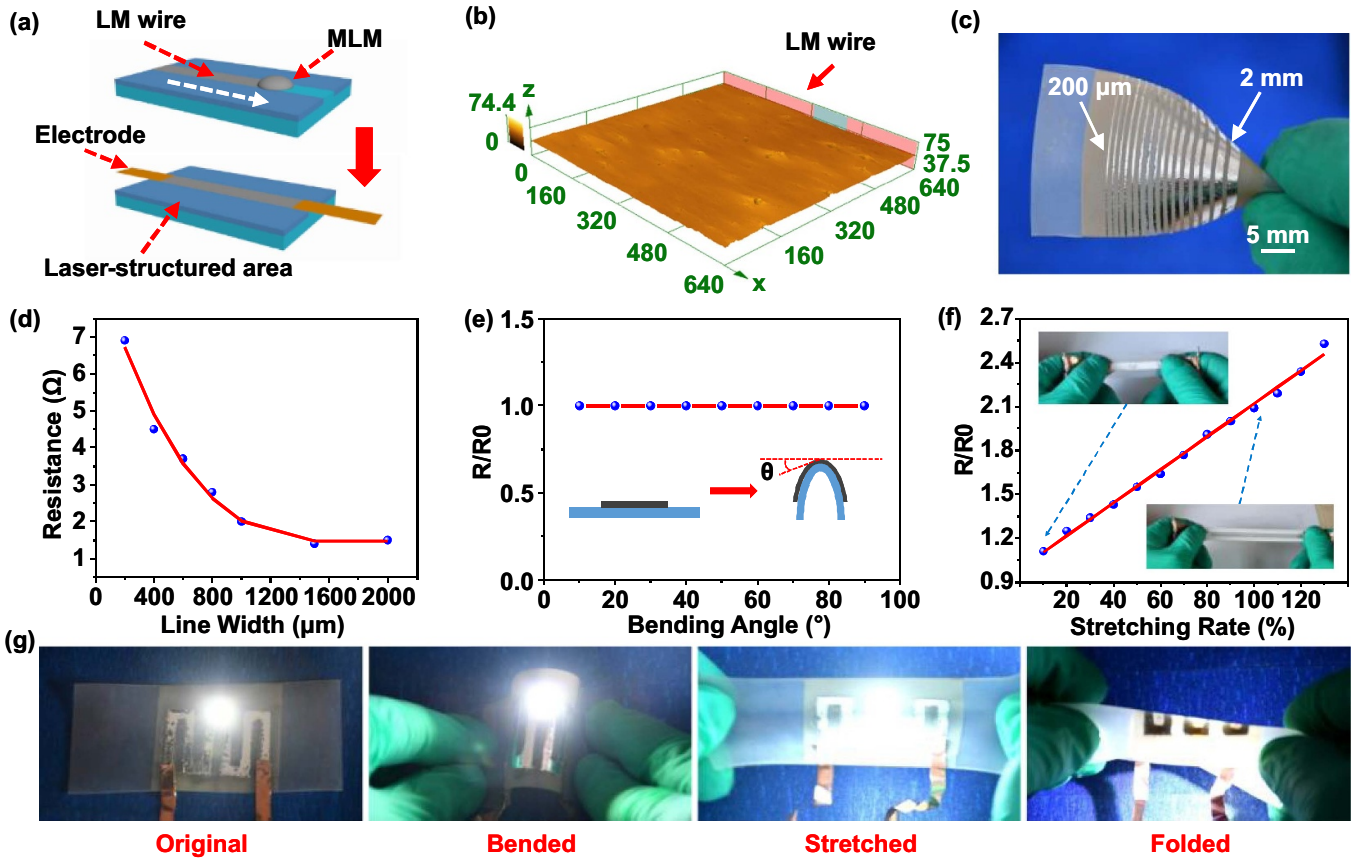

Figure 3. Electrical and flexible properties of the printed LM wire. (a) Process of preparing an LM wire in a circuit. (b) Laser confocal microscopy image of the surface morphology of the printed LM wire. (c) Image of the printed LM lines with different line widths. (d) Relationship between the resistance and the line width of the printed LM lines at a constant length of 15 mm. (e), (f) Influence of (e) the bending treatment and (f) the stretching treatment on the resistance of the LM wire (the initial resistance value ($R0$) is 5.3 Ω). (g) Conductivity test of the printed LM circuit under different deformation conditions.

on the flatness of the printed circuit surface (figure S4, supporting information). When the content of Fe particle was low (wt% = 5%), the surface of the printed LM line was smooth but not flat. The limited Fe particles did not provide enough driving force for the MLM droplet under a magnetic field. Although the MLM droplet moved forward, it did not fully spread on the un-ablated area, resulting in a nonuniform LM line. As the content of Fe particle increased, the printed LM line became thicker. A flat and uniform LM trace with a smooth surface was printed at an Fe particle content of 15%. Figure 3(b) shows the 3D surface morphology of the printed LM wire. The printed LM line had a very low surface roughness of 1.226 μm. On the other hand, the higher content of Fe increased the amount of the Fe particles remaining in the LM trace. When the Fe particle content further increased to 35%, the printed LM line was very flat. However, the surface of the LM line was not smooth because a mass of Fe particles developed on the LM trace. Therefore, the MLM with Fe particle content of 15% is optimal for printing a uniform and consistent conductive line.

The width of the printed LM line can be flexibly designed by the width of the unablated domain. Figure 3(c) shows the image of the printed LM lines with different widths. A minimum line width of 200 μm was realized. These high precision LM lines were prepared in a single printing process. The resistance of the printed LM wire decreases with increasing the line width (figure 3(d)). It is consistent with the resistivity formula, so an LM wire with different resistances can be obtained by designing the width of the LM wire.

Silicone is a flexible substrate, so the LM circuit printed on the silicone surface can be bent and stretched (figure S5, supporting formation). The influence of the bending and stretching treatments on the electrical property (i.e. resistance) of the LM line was investigated. Figure 3(e) shows the resistance change ($R/R0$) of the LM line under different bending angles. $R0$ and R are the resistance of the original LM wire and the deformed LM wire, respectively. The $R/R0$ remained at a constant value as the silicone substrate was bent from 0° to 90°. Under different degrees of bending, the length and the width of the LM wire almost do not change, so the resistance of the LM wire was also unchanged. Conversely, stretching deformation tuned the resistance of the LM wire. The silicone substrate elongates when it is stretched. The resistance of the LM circuit is proportional to the length of the LM wire. Therefore, the resistance of the LM wire increases as the stretch rate (ratio of the stretched length to the original length) increases, as shown in figure 3(f). Most importantly, there is a linear relationship between resistance and stretch rate. Such a change

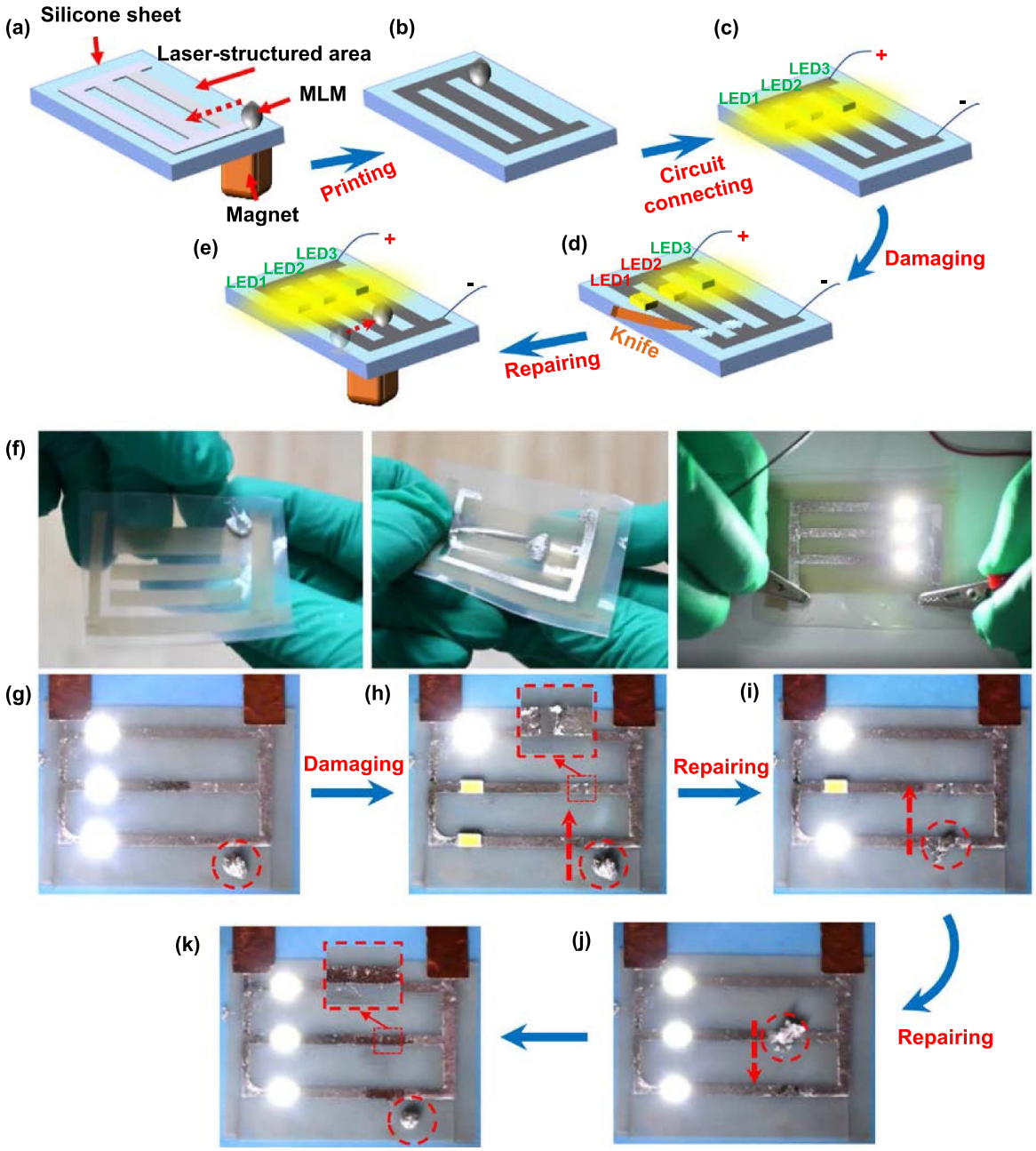

Figure 4. Repairing a printed LM circuit by a magnetic field-controlled MLM droplet. (a)–(e) Schematic of the process of repairing a printed LM circuit: (a) laser patterning, (b) printing LM for preparing an original LM circuit, (c) integration of LED lamps, (d) breaking the LM lines in the circuit, and (e) moving an MLM droplet to the damaged position and reprinting LM onto the broken circuit line. (f) Guiding the MLM to print the LM circuit and connecting the LED lamps. (g)–(k) Experimental result of repairing a damaged LM circuit: (g) connected state of the original LM circuit, (h) damaging the LM wires, (i), (j) controlling an MLM droplet to repair the damaged circuit, and (k) moving the MLM droplet away from the circuit.

trend of resistance enables the use of printed LM wires in stretchable electronic devices, such as tensile sensors. An LED lamp integrated into an LM circuit could stay bright regardless of whether the silicone substrate was bent, stretched, or folded (figure 3(g)). The stable electrical performance allows printed LM circuits to be applied in various flexible wearable electronics.

By taking advantage of the controllable movement of the MLM droplet and its different wetting behaviors on the untreated silicone surface and the laser-structured silicone surface, the MLM droplet can be guided by a magnet to repair a damaged LM circuit. For example, a simple LM circuit was prepared using the abovementioned LM-printing method, including the steps of laser patterning, printing LM, and the integration of LED lamps, as shown in figures 4(a)–(c) and (f). After connecting the circuit, all of the LED lamps lighted (figures 4(c) and (f)). Like a movement-controllable robot, the MLM droplet under the magnetic field can be used to print an LM circuit and repair a damaged LM circuit. As shown in figures 4(d), (g), and (h), once the LM lines in the circuit

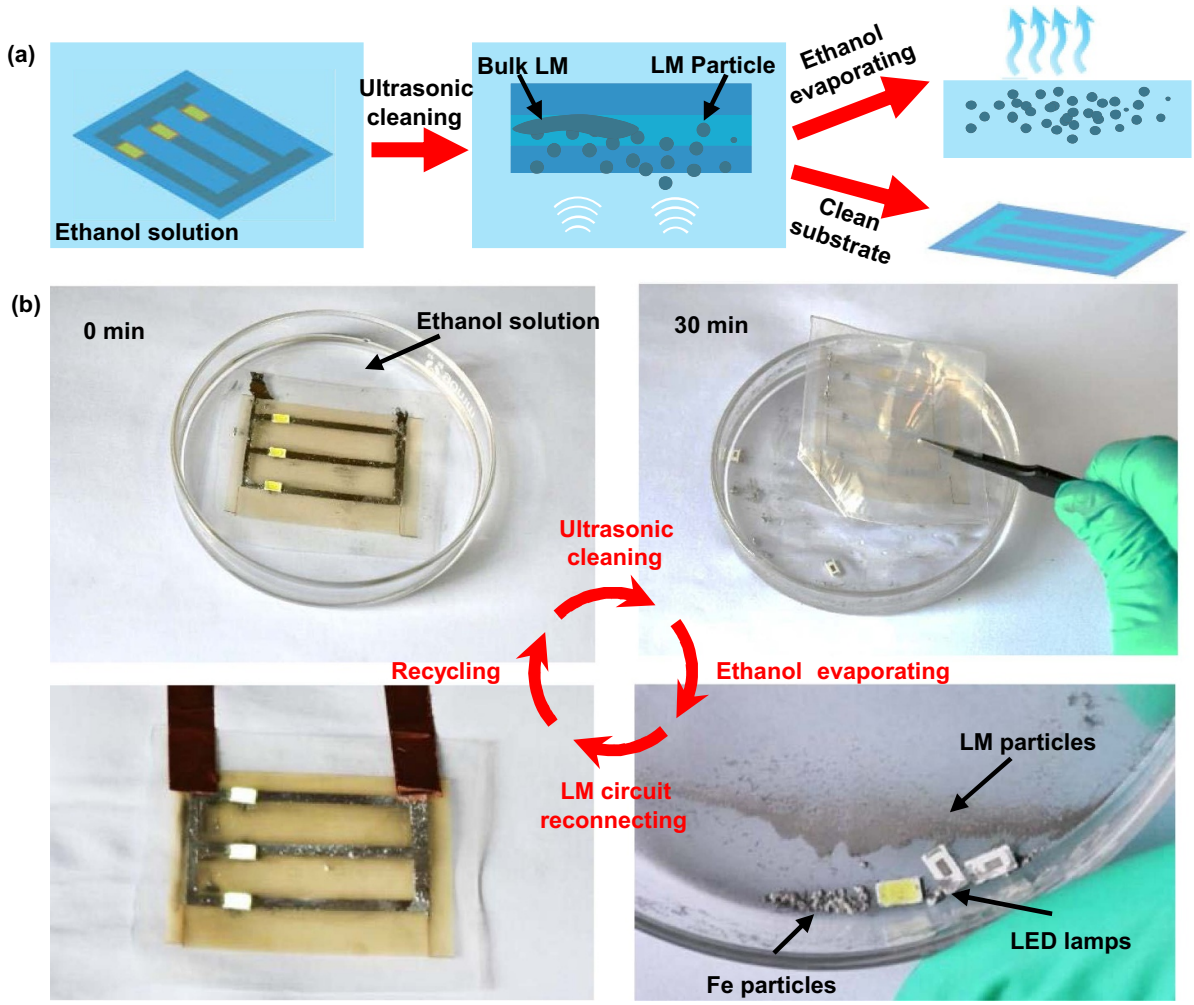

Figure 5. Liquid metal circuit recycling. (a) Schematic process of the recycling the LM circuit. (b) Experimental results of the recycling.

broke, corresponding LED lamps turned off. LM circuits are more vulnerable than rigid metal circuits, so it is necessary to propose a method of repairing LM circuits. Interestingly, the broken circuit could be reconnected by an MLM droplet, which acted as a repair robot. The MLM droplet was guided to the damaged position and reprinted LM onto the broken circuit line (figure 4(e)). Once the LM lines reconnected, the LED lamps lighted again (figures 4(i) and (j)). Finally, the MLM droplet was removed from the circuit (figure 4(k)). The original electrical continuity was not affected by the repair process because the MLM can only leave a mark on the damaged area rather than the surrounding laser-induced supermetalphobic area. Even after many cycles of repairing treatments, the healed circuit line still had the same resistance as the original LM line (figure S6, supporting information). The printing and repairing functions of MLM droplets can ensure a long service lifetime for flexible LM circuits.

LM printed on a laser-patterned substrate can be repaired when broken and fully recycled. Gallium-based alloy is a precious metal, so recycling the wasted materials is particularly important. LM can dissolve in an ethanol solution and thus disperse into microparticles. Those LM particles can be collected after the ethanol solution evaporates. So, the recycled LM can still be reused for printing LM patterns. The LM circuit was ultrasonically cleaned in an alcohol solution for 30 min (figures 5(a) and (b)). The bulk LM adhered on the surface of the laser-patterned substrate dispersed into LM particles and separated from the silicone substrate (figure 5(a)). After the ultrasonic cleaning process, the laser-patterned silicone surface was fully cleaned. Most importantly, the LM particles were completely recycled for reuse after the alcohol evaporated. As shown in figure 5(b), the ultrasonic cleaning was processed only once. A magnet can separate the Fe particles from the LM particles. The microstructures on the recycled silicone substrate maintain great supermetalphobicity. Therefore, the MLM can still be guided to print the LM pattern on the recycled silicone substrate.

Due to their high flexibility and high electrical conductivity, printed LM patterns have potential applications in soft circuits. Since stretching deformation can change the resistance of an LM wire, a flexible tensile sensor was easily prepared, as shown in figure 6(a). A series of LM lines were printed on the laser-patterned silicone substrate (figure 6(b)). Then, the LM circuit was encapsulated in sealing silicone. Figure 6(c) shows the resistance change ($R/R0$) as the tensile sensor was stretched to a different extent and then recovers to its original

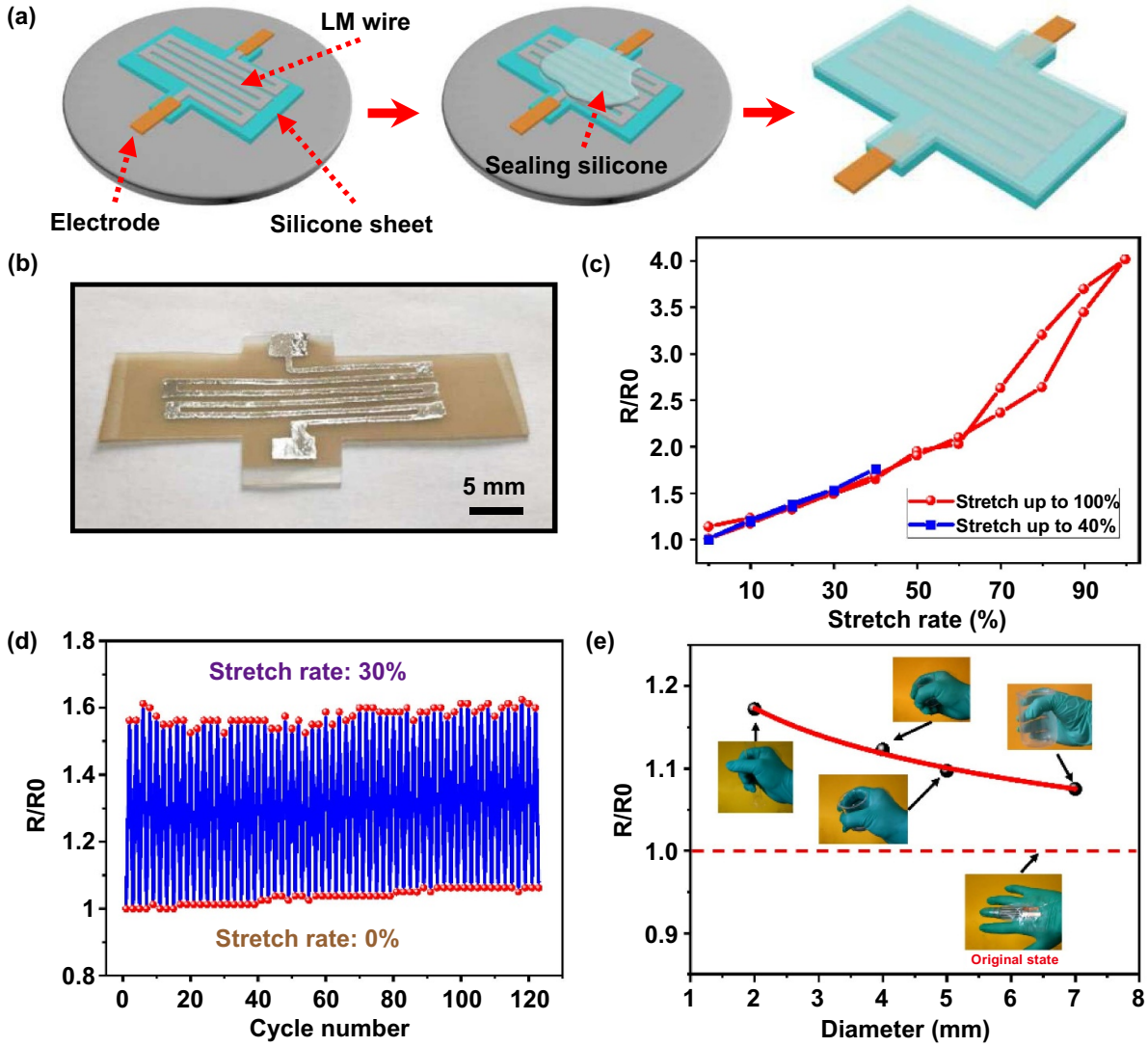

Figure 6. Preparation of a flexible tensile sensor based on the printed LM circuit. (a) Process of preparing a tensile sensor. (b) Image of the printed LM circuit for the tensile sensor. (c) Resistance change of the tensile sensor during a cycle of stretching and recovery. (d) Resistance change of the tensile sensor after repeated stretch. (e) Resistance change of the flexible tensile sensor with the diameter of the held objects for detecting the bending degree of a finger.

state. The initial resistance of the tensile sensor was 8.5 Ω. In a cycle of stretching rate from 0% to 100% and then back to 0%, an obvious hysteresis (maximum value of 10.4 Ω) occurred in the stretch rate range of 60%–100%. By contrast, the resistance changes of the tensile sensor remained stable at a low stretch rate (<60%). When the stretch rate increased from 0% to 40% and then decreased to 0%, the maximum resistance hysteresis of the tensile sensor was only 0.2 Ω during the entire cycle (figure 6(c)). These results indicate that the sensor has good tensile-resistance stability when the stretch rate is less than 60%. Figure 6(d) presents the resistance change of the tensile sensor as it was repeatedly stretched between 0% and 30% for 120 cycles. The *R*/*R*0 value stably switched with the repeated stretching, indicating that the sensor has durable sensing capability.

LM flexible tensile sensors can withstand a large degree of tensile deformation, so they are suitable to be used in wearable devices to detect human behavior. As shown in figure 6(e), when the as-prepared tensile sensor was pasted on the finger, the sensor could detect different bending degrees (i.e. different gestures) of the finger based on the resistance change. Holding objects with different diameters requires the bending the fingers at different degrees. The resistance of the tensile sensor will change according to the diameter of the held object. The resistance change can also reflect the bending degree of the finger as well as the gesture.

4. Conclusions

In conclusion, a method of guiding an MLM droplet by a magnetic field to print and repair a flexible LM circuit on an fs laser-patterned silicone surface was proposed. A microstructure was directly induced on a silicone surface by a single-step fs laser ablation, allowing the silicone surface to greatly repel the MLM. An MLM droplet composed of LM and magnetic

Fe particles was placed on the laser-structured surface and had a CA of 169.5° ± 3.5° and an SA of 5° ± 1°. Based on the selective wetting behavior of the MLM on the laser-structured surface and the unablated smooth surface, LM was easily printed on the laser-induced pattern, generating various smooth, uniform, and high-resolution LM patterns. The printed LM line on the silicone substrate had high flexibility and high electrical conductivity, so it can be used in a soft circuit. The MLM droplet was guided by the magnetic field to repair the damaged LM lines. To save the materials of the LM circuit, the wasted and broken LM circuit can be recycled in an alcohol solution for subsequent printing. Furthermore, the recycled silicone substrate omits the laser ablation process, which lowers processing costs. A flexible tensile sensor was prepared based on the printed LM circuit, which could detect the bending degree of a finger. The laser-patterned method under a magnetic field allows for more flexibile and functional LM manipulation, which has great significance for exploring soft circuits in the furture.

Acknowledgments

This work is supported by the National Science Foundation of China under the Grant No. 61875158, the National Key Research and Development Program of China under the Grant No. 2017YFB1104700, the International Joint Research Laboratory for Micro/Nano Manufacturing and Measurement Technologies, and the Fundamental Research Funds for the Central Universities.

Conflict of interest

The authors declare no conflict of interest.

ORCID iD

Feng Chen https://orcid.org/0000-0002-7031-7404

References

[1] Biswas S, Schoeberl A, Hao Y F, Reiprich J, Stauden T, Pezoldt J and Jacobs H O 2019 Integrated multilayer stretchable printed circuit boards paving the way for deformable active matrix *Nat. Commun.* **10** 4909
[2] Kim S Y, Baines R, Booth J, Vasios N, Bertoldi K and Kramer-Bottiglio R 2019 Reconfigurable soft body trajectories using unidirectionally stretchable composite laminae *Nat. Commun.* **10** 3464
[3] Wang S *et al* 2018 Skin electronics from scalable fabrication of an intrinsically stretchable transistor array *Nature* **555** 83–88
[4] Shintake J, Cacucciolo V, Floreano D and Shea H 2018 Soft robotic grippers *Adv. Mater.* **30** 1707035
[5] Choi S, Han S I, Kim D, Hyeon T and Kim D H 2019 High-performance stretchable conductive nanocomposites: materials, processes, and device applications *Chem. Soc. Rev.* **48** 1566–95
[6] Kamyshny A and Magdassi S 2019 Conductive nanomaterials for 2D and 3D printed flexible electronics *Chem. Soc. Rev.* **48** 1712–40
[7] Liu Y, Wang H, Zhao W, Zhang M, Qin H B and Xie Y Q 2018 Flexible, stretchable sensors for wearable health monitoring: sensing mechanisms, materials, fabrication strategies and features *Sensors* **18** 645
[8] Ko S H, Pan H, Grigoropoulos C P, Luscombe C K, Fréchet J M J and Poulikakos D 2007 All-inkjet-printed flexible electronics fabrication on a polymer substrate by low-temperature high-resolution selective laser sintering of metal nanoparticles *Nanotechnology* **18** 345202
[9] Kwon J, Cho H, Suh Y D, Lee J, Lee H, Jung J, Kim D, Lee D, Hong S and Ko S H 2017 Flexible and transparent cu electronics by low-temperature acid-assisted laser processing of Cu nanoparticles *Adv. Mater. Technol.* **2** 1600222
[10] Kwon J, Suh Y D, Lee J, Lee P, Han S, Hong S, Yeo J Lee H and Ko S H 2018 Recent progress in silver nanowire based flexible/wearable optoelectronics *J. Mater. Chem.* C **6** 7445–61
[11] Won P, Park J J, Lee T, Ha I, Han S, Choi M, Lee J, Hong S, Cho K J and Ko S H 2019 Stretchable and transparent kirigami conductor of nanowire percolation network for electronic skin applications *Nano Lett.* **19** 6087–96
[12] Wang Y *et al* 2017 A highly stretchable, transparent, and conductive polymer *Sci. Adv.* **3** e1602076
[13] Jin Y, Lin Y L, Kiani A, Joshipura I D, Ge M Q and Dickey M D 2019 Materials tactile logic via innervated soft thermochromic elastomers *Nat. Commun.* **10** 4187
[14] Li X K, Li M J, Xu J, You J, Yang Z Q and Li C X 2019 Evaporation-induced sintering of liquid metal droplets with biological nanofibrils for flexible conductivity and responsive actuation *Nat. Commun.* **10** 3514
[15] Ota H, Chen K, Lin Y J, Kiriya D, Shiraki H, Yu Z B, Ha T J and Javey A 2014 Highly deformable liquid-state heterojunction sensors *Nat. Commun.* **5** 5032
[16] Yun G, Tang S Y, Sun S S, Yuan D, Zhao Q B, Deng L, Yan S, Du H P, Dickey M D and Li W H 2019 Liquid metal-filled magnetorheological elastomer with positive piezoconductivity *Nat. Commun.* **10** 1300
[17] Markvicka E J, Bartlett M D, Huang X N and Majidi C 2018 An autonomously electrically self-healing liquid metal-elastomer composite for robust soft-matter robotics and electronics *Nat. Mater.* **17** 618–24
[18] Yan J J, Malakooti M H, Lu Z, Wang Z Y, Kazem N, Pan C F, Bockstaller M R, Majidi C and Matyjaszewski K 2019 Solution processable liquid metal nanodroplets by surface-initiated atom transfer radical polymerization *Nat. Nanotechnol.* **14** 684–90
[19] Gu L L *et al* 2020 A biomimetic eye with a hemispherical perovskite nanowire array retina *Nature* **581** 278–82
[20] Dickey M D 2017 Stretchable and soft electronics using liquid metals *Adv. Mater.* **29** 1606425
[21] Gao Y J *et al* 2017 Wearable microfluidic diaphragm pressure sensor for health and tactile touch monitoring *Adv. Mater.* **29** 1701985
[22] Gao Y J, Yu L T, Yeo J C and Lim C T 2020 Flexible hybrid sensors for health monitoring: materials and mechanisms to render wearability *Adv. Mater.* **32** 1902133
[23] Hirsch A, Michaud H O, Gerratt A P, De Mulatier S and Lacour S P 2016 Intrinsically stretchable biphasic (solid-liquid) thin metal films *Adv. Mater.* **28** 4507–12
[24] Park S, Thangavel G, Parida K, Li S H and Lee P S 2019 A stretchable and self-healing energy storage device based on mechanically and electrically restorative liquid-metal particles and carboxylated polyurethane composites *Adv. Mater.* **31** 1805536

[25] Lu T, Markvicka E J, Jin Y C and Majidi C 2017 Soft-matter printed circuit board with UV laser micropatterning *ACS Appl. Mater. Interfaces* **9** 22055–62
[26] Lu T, Wissman J, Ruthika and Majidi C 2015 Soft anisotropic conductors as electric vias for Ga-based liquid metal circuits *ACS Appl. Mater. Interfaces* **7** 26923–9
[27] Daeneke T, Khoshmanesh K, Mahmood N, De Castro I A, Esrafilzadeh D, Barrow S J, Dickey M D and Kalantar-Zadeh K 2018 Liquid metals: fundamentals and applications in chemistry *Chem. Soc. Rev.* **47** 4073–111
[28] Hirsch A, Dejace L, Michaud H O and Lacour S P 2019 Harnessing the rheological properties of liquid metals to shape soft electronic conductors for wearable applications *Acc. Chem. Res.* **52** 534–44
[29] Gheribi A E and Chartrand P 2019 Temperature and oxygen adsorption coupling effects upon the surface tension of liquid metals *Sci. Rep.* **9** 7113
[30] Zhang W *et al* 2015 Liquid metal/metal oxide frameworks with incorporated Ga_2O_3 for photocatalysis *ACS Appl. Mater. Interfaces* **7** 1943–8
[31] Li Q, Lin J, Liu T Y, Dong S J, Zheng H and Liu J 2020 Supermetallophobic functional coatings based on silicate clays and a method to pattern liquid metals *ACS Appl. Electron. Mater.* **2** 2229–41
[32] Chen Z Y and Lee J B 2019 Surface modification with gallium coating as nonwetting surfaces for gallium-based liquid metal droplet manipulation *ACS Appl. Mater. Interfaces* **11** 35488–95
[33] Kalantar-Zadeh K, Tang J B, Daeneke T, O'Mullane A P, Stewart L A, Liu J, Majidi C, Ruoff R S, Weiss P S and Dickey M D 2019 Emergence of liquid metals in nanotechnology *ACS Nano* **13** 7388–95
[34] Malakooti M H, Kazem N, Yan J J, Pan C F, Markvicka E J, Matyjaszewski K and Majidi C 2019 Liquid metal supercooling for low-temperature thermoelectric wearables *Adv. Funct. Mater.* **29** 1906098
[35] Sivan V, Tang S Y, O'Mullane A P, Petersen P, Eshtiaghi N, Kalantar-Zadeh K and Mitchell A 2013 Liquid metal marbles *Adv. Funct. Mater.* **23** 144–52
[36] Handschuh-Wang S, Chen Y Z, Zhu L F and Zhou X C 2018 Analysis and transformations of room-temperature liquid metal interfaces-a closer look through interfacial tension *ChemPhysChem* **19** 1584–92
[37] Guo R, Cui B X, Zhao X J, Duan M H, Sun X Y, Zhao R Q, Sheng L, Liu J and Lu J 2020 Cu–EGaIn enabled stretchable e-skin for interactive electronics and CT assistant localization *Mater. Horiz.* **7** 1845–53
[38] Wang Q, Yu Y, Yang J and Liu J 2015 Fast fabrication of flexible functional circuits based on liquid metal dual-trans printing *Adv. Mater.* **27** 7109–16
[39] Dejace L, Laubeuf N, Furfaro I and Lacour S P 2019 Gallium-based thin films for wearable human motion sensors *Adv. Intell. Syst.* **1** 1900079
[40] Ma B, Xu C T, Chi J J, Chen J, Zhao C and Liu H 2019 A versatile approach for direct patterning of liquid metal using magnetic field *Adv. Funct. Mater.* **29** 1901370
[41] Cao L X, Yu D H, Xia Z S, Wan H Y, Liu C K, Yin T and He Z Z 2020 Ferromagnetic liquid metal putty-like material with transformed shape and reconfigurable polarity *Adv. Mater.* **32** 2000827
[42] Zheng Y, He Z Z, Gao Y X and Liu J 2013 Direct desktop printed-circuits-on-paper flexible electronics *Sci. Rep.* **3** 1786
[43] Zheng Y, He Z Z, Yang J and Liu J 2014 Personal electronics printing via tapping mode composite liquid metal ink delivery and adhesion mechanism *Sci. Rep.* **4** 4588
[44] Deng B W and Cheng G J 2019 Pulsed laser modulated shock transition from liquid metal nanoparticles to mechanically and thermally robust solid-liquid patterns *Adv. Mater.* **31** 1807811
[45] Bandodkar A J, Nuñez-Flores R, Jia W Z and Wang J 2015 All-printed stretchable electrochemical devices *Adv. Mater.* **27** 3060–5
[46] Abbasi R *et al* 2020 Photolithography–enabled direct patterning of liquid metals *J. Mater. Chem.* C **8** 7805–11
[47] Merhebi S *et al* 2020 Magnetic and conductive liquid metal gels *ACS Appl. Mater. Interfaces* **12** 20119–28
[48] Guo R, Sun X Y, Yuan B, Wang H Z and Liu J 2019 Magnetic liquid metal (Fe-EGaIn) based multifunctional electronics for remote self-healing materials, degradable electronics, and thermal transfer printing *Adv. Sci.* **6** 1901478
[49] Luebbers P R and Chopra O K 1995 Compatibility of ITER candidate materials with static gallium *Proc. 16th Int. Symp. on Fusion Engineering (30 September–5 October 1995, Champaign, IL)* (Piscataway, NJ: IEEE) pp 232–5
[50] Zhang D S, Wu L C, Ueki M, Ito Y and Sugioka K 2020 Femtosecond laser shockwave peening ablation in liquids for hierarchical micro/nanostructuring of brittle silicon and its biological application *Int. J. Extreme Manuf.* **2** 045001
[51] Zhang D S, Ranjan B, Tanaka T and Sugioka K 2020 Underwater persistent bubble-assisted femtosecond laser ablation for hierarchical micro/nanostructuring *Int. J. Extreme Manuf.* **2** 015001
[52] Yong J L, Bai X, Yang Q, Hou X and Chen F 2021 Filtration and removal of liquid polymers from water (polymer/water separation) by use of the underwater superpolymphobic mesh produced with a femtosecond laser *J. Colloid Interface Sci.* **582** 1203–12
[53] Fang Y, Liang J, Bai X, Yong J L, Huo J L, Yang Q, Hou X and Chen F 2020 Magnetically controllable isotropic/anisotropic slippery surface for flexible droplet manipulation *Langmuir* **36** 15403–9
[54] Zhang C J, Yang Q, Shan C, Zhang J Z, Yong J L, Fang Y, Hou X and Chen F 2020 Tuning a surface super-repellent to liquid metal by a femtosecond laser *RSC Adv.* **10** 3301–6
[55] Yong J L, Zhang C J, Bai X, Zhang J Z, Yang Q, Hou X and Chen F 2020 Designing 'supermetalphobic' surfaces that greatly repel liquid metal by femtosecond laser processing: does the surface chemistry or microstructure play a crucial role? *Adv. Mater. Interfaces* **7** 1901931